Investigating the effects of clustering in a laser wakefield accelerator

Contact: savio.rozario11@imperial.ac.uk

S. V. Rozario, E. Gerstmayr, J. M. Cole, N. Lopes, K. Poder, J. C. Wood, S. P. D. Mangles, Z. Najmudin
The John Adams Institute for Accelerator Science
Blackett Laboratory,
Imperial College London,
SW7 2AZ, UK

L.Wilson, D. Rusby, E. Zemaityte, D. Neely
Central Laser Facility, STFC,
Rutherford Appleton Laboratory,
Didcot, OX11 0QX, UK

D. Symes, N. Booth, N. Bourgeois, O. Chekhlov, S. Hawkes, C. Hooker, R. Pattathil
Central Laser Facility, STFC,
Rutherford Appleton Laboratory,
Didcot, OX11 0QX, UK

S. Dorking, D. Lockley, G. Cook, R. Deas
DSTL, Porton Down,
Salisbury, Wiltshire, SP4 0JQ

1 Introduction

Laser wakefield acceleration is a rapidly maturing particle acceleration technique which is used to generate particle beams using laser-matter interactions [1]. This method has the distinct advantage that it can sustain acceleration gradients several orders of magnitude (100s $GV\,m^{-1}$) greater than conventional RF cavities (≤ 100 $MV\,m^{-1}$), making the accelerator much more compact. This rapidly developing field has already been used for a number applications e.g generating hard x-rays for absorption contrast imaging [2].

One aspect of Laser wakefield accelerators (LWFAs) which is being actively researched is the stability of the generated electron beams. Control over these electron beams will increase the scope of applications for LWFA. Since narrow energy spread beams were first achieved through the self-injection mechanism [3–5], several types of injection mechanisms have been proposed to control the parameters of the electron beam. Here we report on an experiment using the Gemini (TA2) laser to investigate injection using the ionisation of clusters [6].

2 Injection

LWFA are driven by a short pulse (<50 fs) high power ($a_0 > 1$) laser to generate a high amplitude electron plasma wave. Where a_0, the normalized vector potential is defined as $a_0 = 0.855(I[10^{18}W/cm^2]\lambda_{\mu m}^2)^{0.5}$. Electrons which are injected into the plasma wave are accelerated by its intrinsic space charge force to high energies. These waves have a phase velocity given by

$$\gamma_p = \frac{n_c}{n_e} \qquad (1)$$

For injection to occur, electrons have to be trapped in the potential of the plasma wave. This can occur for a sufficiently non-linear plasma wave if stationary electrons are present near the minimum of the wake potential. The minimum a_0 require to trap stationary electrons is given as [7]

$$a_0 \gtrsim 1.2\sqrt{1 - \gamma_p^{-1}}$$

3 Cluster dynamics

A cluster is a collection of atom/molecules ranging from 10s to 10,000s of particles at solid density. Clustering is achieved by using a supersonic gas jet [8]. As the gas exits the nozzle its flow velocity increases while its flow temperature decreases. This triggers the onset of clusters inside a gas. The van-der Waals force in a cluster holds the atoms together at solid density. This effect is typically parametrised by an empirical scaling law named the Hagena parameter (Γ^*) [9].

$$\Gamma^* = k\frac{(d/\tan(\alpha))^{0.85}}{T_0^{2.29}}P_0$$
$$N_A = \Gamma^{*2}$$

In this expression d is the throat diameter of the gas jet (in mm), α is the expansion half angle of the gas jet, T_0 is the temperature of the reservoir, P_0 is the backing pressure of the gas jet, k is a value which depends on the gas used and N_A is the average number of atoms in the cluster. For $\Gamma^* > 100$ the medium is known to cluster [8]. The value of k for a particular species in this expression has been determined experimentally. For the gases used in this experiment, the relevant values are shown in Table 1

	helium	methane
k	3.85	2360

Table 1: Values of k for the gases used in this experiment [8]

4   Cluster injection

Clusters provide a much larger source of stationary electrons. It is hypothesized that they will increase the charge of the electron beam injected into the plasma wave. In Figure 1 it can be seen that the electrons which are liberated near the peak of the laser pulse (and subsequently near the minimum of the potential of the plasma wave) are the ones being trapped are accelerated.
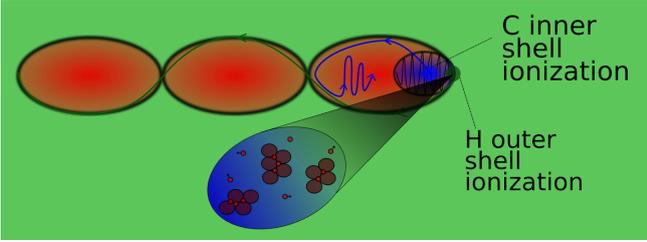

Figure 1: Blue path represents the path taken by electrons which are injected by cluster enhanced ionisation injection.
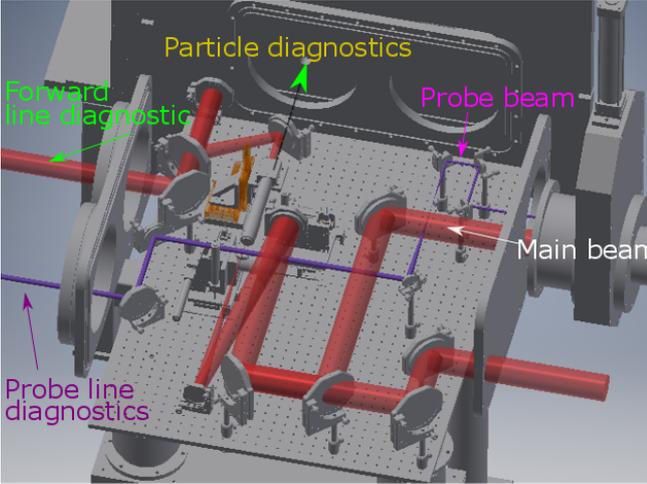
5   Experimental setup

Figure 2: Experiment layout

The Gemini (TA2) laser was used to carry out this experiment. This laser provides 500 ± 5 mJ pulse in 45 ± 5 fs focused onto a 15 ± 5 µm spot size using a $f/17$ focusing geometry as can be seen in Figure 2.

The generated electron beam is diagnosed using two diagnostics, namely the beam profile monitor which is a scintillating sheet of Lanex (L1 in Figure 3) normal to the electron beam and the electron spectrometer which consists of a 0.6 T magnet and two Lanex screens (L2 and L3 in Figure 3) to capture low energy (10 - 45 MeV) and high energy (45 - 300 MeV) electrons.

The beam profile monitor is at the entrance of the electron spectrometer and this provides additional information about the pointing of the electron beam into the spectrometer as can be seen in Figure 3. The measured
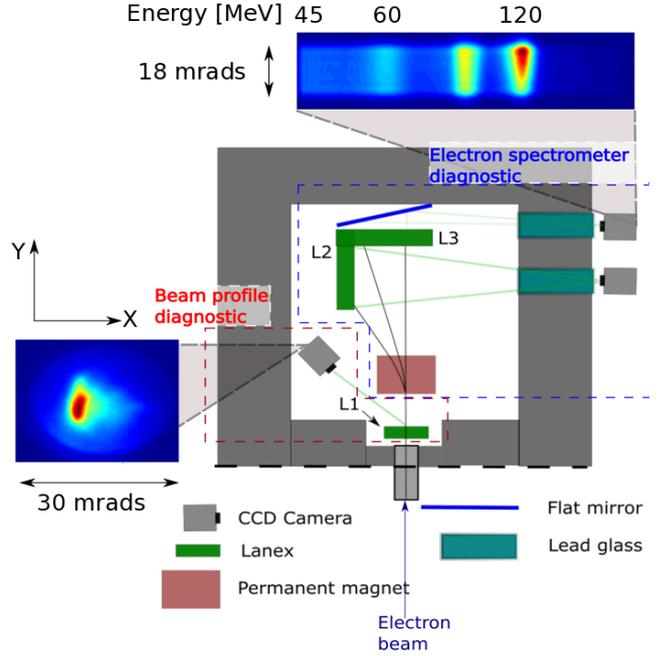

Figure 3: Particle diagnostics layout

charge was absolutely calibrated on the high energy electron spectrometer. This was done by using image plate (IP) and then calibrating the counts on the camera to the charge retrieved using IP [10]. The charge on the other two lanex screens for the beam profile monitor and the lower energy electron spectrometer could be inferred relative to the high energy electron spectrometer.

Two main types of targetry are used in this experiment, a 5mm exit diameter gas jet and a variable length (3-7 mm) gas cell (see Figure 4). In a gas cell, the conditions for clustering (the gas cell is filled slowly and the fluid does not undergo cooling) is not present.

The gas cell will have a different scale length for its ramp compared to a gas jet. To identify this effect, helium was also examined in the gas cell compared to the gas jet. Density was measured using a Mach-Zender interferometer and verified using fluid simulations performed using the FLASH hydrodynamic code[11]. Fluid codes provide the mass density (ρ) of a gaseous species, by assuming an ionisation state (Z) we obtain the electron number density (n_e) in the plasma channel.

$$n_e = \frac{\rho Z}{m_s} \qquad (2)$$

By varying the inlet gas pressure we could control the electron number density of the interaction. The electron number densities range of interest is 5×10^{18}cm^{-3} - 4.5×10^{19}cm^{-3}

Where m_s is the mass of a single molecule or atom. Methane from a high pressure gas jet was used as the target gas for testing the effects of clustering. Hence by comparing the difference between methane in these two settings it is possible to discern the effect of clustering on LWFA.
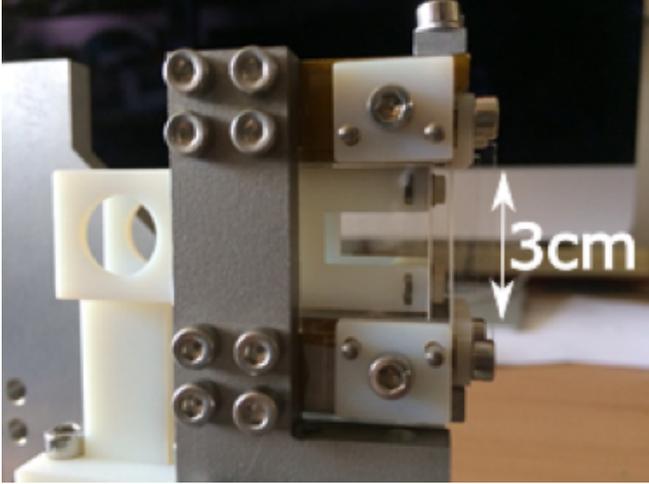

Figure 4: Gas cell used in this experiment

6 Charge enhancement from clustering

Methane in a gas cell configuration (where clustering does not occur) was compared to the gas jet case (where clustering occurs) for similar plasma lengths. The mean laser energy for clustered case was 510 ± 40 mJ and for the non-clustered case is 540 ± 40 mJ.
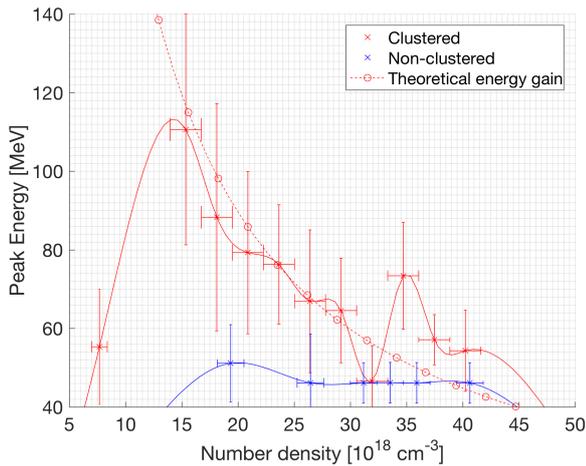

Figure 5: Peak electron energy. The linear 1D energy gain is given by $W_{\max}[\mathrm{eV}] = \frac{2m_e c^2 n_c}{n_e}$

In Figure 5, the clustered case can be seen to follows the 1D energy scaling within the error bars, whereas the non-clustered case does not.
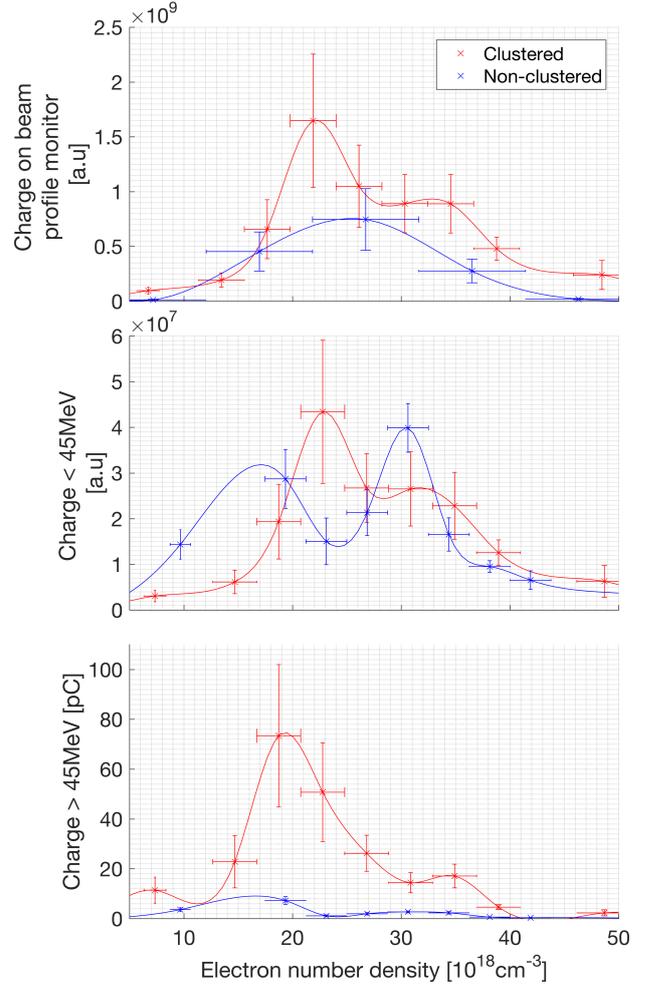

Figure 6: Comparison of beam charge between the clustered (red) & non-clustered (blue) on a) Beam profile monitor, b) Low energy electron spectrometer and c) High energy electron spectrometer.

In Figure 6a it can be seen that for the clustered medium the charge on the beam profile monitor is significantly higher than the non-clustered case.

	Clustered	Non-clustered
X Pointing [mrads]	1.46 ± 0.18	1.56 ± 0.36
Y Pointing [mrads]	1.84 ± 0.22	2.69 ± 0.49
Short axis beam divergence [mrads]	7.29 ± 0.72	7.51 ± 1.02
Long axis beam divergence [mrads]	9.44 ± 0.66	10.63 ± 1.61
Γ^*	143-448	N/A
Mean cluster size	5.4×10^4-6.8×10^5	N/A

Table 2: Electron beam and cluster properties

7 Discussion

It can be seen in Figure 6a that the charge of the electron beam incident on the beam profile monitor is greater, by a factor of up to 2, for the case where clustering is present relative to the case where clustering is absent.

Within the spectral fluctuations, it can be see the low energy part of the spectrum (defined as being less than 45 MeV) in Figure 6b does not gain a significant amount of charge between the two cases.

The charge enhancement affects the high energy part of the spectrum of the electron beam more than the lower energy part of the spectrum. The relative difference in charge between the clustered/non-clustered in the high energy lanex screen is up to 35 times in Figure 6c.

The electron beam for the non-clustered case is on the threshold of detection for the high energy lanex ($\leq$ 45MeV) which is why they are not observed on the lanex screens. The electron beams generated by a clustered plasma reach significantly higher energies than in non-clustered plasma. This could also be because of guiding enhancement in a clustered plasma [13].

When the laser pulse is being guided more efficiently in the medium, it can maintain high enough intensities to drive a plasma wave for greater distances. The plasma wave needs to be driven for long enough such than electrons can gain energy from it. This is the reason why the clustered case follows the linear 1D energy scaling whereas the non-clustered case does not.

8 Conclusion

The presence of clustering can be seen to increase the charge injected into a wakefield accelerator. This is attributed to the injection of electrons from solid density clusters in plasma. Clustering also influences the peak energy that the electron beams reach after being injected. Enhancements in the guiding of the laser pulse are purported to influence the peak electron energy.

9 Acknowledgements

References

[1] T. Tajima and J. M. Dawson. Laser electron accelerator. *Physical Review Letters*, 43(4):267–270, 1979.

[2] J M Cole, J C Wood, N C Lopes, et al. Laser-wakefield accelerators as hard x-ray sources for 3D medical imaging of human bone. *Scientific reports*, 5:13244, 2015.

[3] C G R Geddes, C S Toth, J Van Tilborg, et al. A laser plasma accelerator producing monoenergetic electron beams. *Nature*, 431(7008):538–541, 2004.

[4] J. Faure, Y. Glinec, A. Pukhov, et al. A laser plasma accelerator producing monoenergetic electron beams. *Nature*, 431(September):541–544, 2004.

[5] S P D Mangles, C D Murphy, Z Najmudin, et al. Monoenergetic beams of relativistic electrons from intense laser-plasma interactions. *Nature*, 431(7008):535–538, 2004.

[6] J. C. Wood. *Betatron Radiation from Laser Wakefield Accelerators and its Applications*. PhD thesis, Imperial College London, 2017.

[7] M. Chen, E. Esarey, C. B. Schroeder, C. G R Geddes, and W. P. Leemans. Theory of ionization-induced trapping in laser-plasma accelerators. *Physics of Plasmas*, 19(3), 2012.

[8] R. A Smith, T Ditmire, and J. W. G Tisch. Characterization of a cryogenically cooled high-pressure gas jet for laser/cluster interaction experiments. *Review of Scientific Instruments*, 69(11):3798, 1998.

[9] O. F. Hagena. Cluster Formation in Expanding Supersonic Jets: Effect of Pressure, Temperature, Nozzle Size, and Test Gas. *The Journal of Chemical Physics*, 56(5):1793, 1972.

[10] A. Buck, K. Zeil, A. Popp, et al. Absolute charge calibration of scintillating screens for relativistic electron detection. *Review of Scientific Instruments*, 81(3), 2010.

[11] Anshu Dubey, Katie Antypas, Murali K. Ganapathy, et al. Extensible component-based architecture for FLASH, a massively parallel, multiphysics simulation code. *Parallel Computing*, 35(10-11):512–522, 2009.

[12] I Alexeev, T. Antonsen, K. Kim, and H. Milchberg. Self-Focusing of Intense Laser Pulses in a Clustered Gas. *Physical Review Letters*, 90(10):103402, 2003.

[13] T Ditmire, R A Smith, and M H Hutchinson. Plasma waveguide formation in predissociated clustering gases. *Opt Lett*, 23(5):322–324, 1998.